


RESEARCH ARTICLE

Tissue engineered nigrostriatal pathway for treatment of Parkinson's disease

Laura A. Struzyna^{1,2,3}  | Kevin D. Browne^{1,2} | Zachary D. Brodrik⁴ | Justin C. Burrell^{1,2,3} | James P. Harris^{1,2} | H. Isaac Chen^{1,2} | John A. Wolf^{1,2} | Kate V. Panzer³ | James Lim^{1,2} | John E. Duda^{2,5} | Rodrigo A. España⁴ | D. Kacy Cullen^{1,2,3}

¹Center for Brain Injury & Repair, Department of Neurosurgery, Perelman School of Medicine, University of Pennsylvania, Philadelphia, PA, USA

²Center for Neurotrauma, Neurodegeneration & Restoration, Corporal Michael J. Crescenz Veterans Affairs Medical Center, Philadelphia, PA, USA

³Department of Bioengineering, School of Engineering and Applied Science, University of Pennsylvania, Philadelphia, PA, USA

⁴Department of Neurobiology & Anatomy, College of Medicine, Drexel University, Philadelphia, PA, USA

⁵Department of Neurology, Perelman School of Medicine, University of Pennsylvania, Philadelphia, PA, USA

Correspondence

D. Kacy Cullen, 105E Hayden Hall/3320 Smith Walk, Dept. of Neurosurgery, University of Pennsylvania, Philadelphia, PA 19104, USA. Email: dkacy@pennmedicine.upenn.edu

Funding information

National Institutes of Health, Grant/Award Numbers: T32-NS091006, T32-NS043126, R01-DA031900, F31-DA042505 and U01-NS094340; Department of Veterans Affairs, Grant/Award Number: I01-BX003748; National Science Foundation, Grant/Award Number: DGE-1321851; University of Pennsylvania, Grant/Award Number: Penn Medicine Neuroscience Pilot Award; Michael J. Fox Foundation, Grant/Award Number: Therapeutic Pipeline Program #9998

Abstract

The classic motor deficits of Parkinson's disease are caused by degeneration of dopaminergic neurons in the substantia nigra pars compacta, resulting in the loss of their long-distance axonal projections that modulate the striatum. Current treatments only minimize the symptoms of this disconnection as there is no approach capable of replacing the nigrostriatal pathway. We are applying microtissue engineering techniques to create living, implantable constructs that mimic the architecture and function of the nigrostriatal pathway. These constructs consist of dopaminergic neurons with long axonal tracts encased within hydrogel microcolumns. Microcolumns were seeded with dopaminergic neuronal aggregates, while lumen extracellular matrix, growth factors, and end targets were varied to optimize cytoarchitecture. We found a 10-fold increase in axonal outgrowth from aggregates versus dissociated neurons, resulting in remarkable axonal lengths of over 6 mm by 14 days and 9 mm by 28 days *in vitro*. Axonal extension was also dependent upon lumen extracellular matrix, but did not depend on growth factor enrichment or neuronal end target presence. Evoked dopamine release was measured via fast scan cyclic voltammetry and synapse formation with striatal neurons was observed *in vitro*. Constructs were microinjected to span the nigrostriatal pathway in rats, revealing survival of implanted neurons while maintaining their axonal projections within the microcolumn. Lastly, these constructs were generated with dopaminergic neurons differentiated from human embryonic stem cells. This strategy may improve Parkinson's disease treatment by simultaneously replacing lost dopaminergic neurons in the substantia nigra and reconstructing their long-projecting axonal tracts to the striatum.

KEYWORDS

dopaminergic neurons, nigrostriatal pathway, Parkinson's disease, regenerative medicine, tissue engineering

1 | INTRODUCTION

Parkinson's disease is a progressive neurodegenerative disease that affects 1–2% of people over 65, causing significant morbidity across a prolonged and escalating disease course. Parkinson's disease is characterized by resting tremor, bradykinesia, rigidity, and other symptoms

that decrease quality of life, ultimately leading to significant disability via the inability to control motor function (Davie, 2008). The motor symptoms of Parkinson's disease are due to the selective loss of dopaminergic neurons in the substantia nigra pars compacta (SNpc). As SNpc neurons send long-projecting axons to the striatum, this stereotypical neurodegeneration deprives the striatum of crucial

dopaminergic inputs and thereby renders an important motor feedback pathway ineffective.

Although several Parkinson's disease treatments have been developed, most options focus on mitigating symptoms resulting from the neurodegeneration of the dopaminergic neurons rather than treating the underlying pathology itself. Dopamine replacement therapies, including 3,4-dihydroxy-L-phenylalanine (L-DOPA) and dopamine agonists, attempt to correct the underproduction of dopamine due to neuron/axon loss (Davie, 2008). These dopamine-related therapies provide symptom improvements, but side effects, such as dyskinesias and motor fluctuations, may develop and efficacy declines over time (Katzenschlager & Lees, 2002). Alternatively, surgery can be performed to implant deep brain stimulation (DBS) systems that modulate basal ganglia network function to alleviate motor symptoms. Although DBS improves motor function, electrode stimulation can have unwanted side effects impacting cognition and speech (Moro et al., 2010). Similar to pharmaceutical therapies, DBS efficacy decreases over time as the disease progression continues. Newer treatments have focused on neuroprotection, but trials have only slightly slowed progression of symptoms (Obeso et al., 2010). Even if an effective neuroprotective treatment could be developed, the treatment could not replace the $\geq 60\%$ of SNpc neurons and their axonal projections to the striatum that have already degenerated by the time of symptom onset (Dauer & Przedborski, 2003).

To address the stereotypical neurodegeneration of Parkinson's disease, significant effort has been focused on replacing components of the nigrostriatal pathway via (a) tissue grafts, (b) cell implantation, and (c) scaffold-based methods. Trials have indicated beneficial functional results from tissue grafts when methods sustain a novel population of at least 80,000 dopaminergic neurons (Bjorklund & Lindvall, 2000). However, although grafts and cells implanted into the striatum create new "factories" for dopamine, these cells do not reconstruct the nigrostriatal pathway and thus lack normal feedback signals that target the SNpc. As a result, striatal neurons still do not receive appropriately timed dopamine signals (Freed et al., 2001; Kim, 2011; Olanow, Freeman, & Kordower, 2001; Redmond Jr, Sladek, & Spencer, 2001). Alternatively, implantations into the SNpc have largely failed because axonal regrowth to the striatum is limited and techniques to coax axonal outgrowth do not ensure specific outgrowth to the correct and/or distant target(s) (Grealish et al., 2014; Nikkhah, Cunningham, Cenci, McKay, & Bjorklund, 1995; Thompson, Grealish, Kirik, & Bjorklund, 2009). Stem cell implantations have been limited by cell loss, nonspecific cell type differentiation, and neoplastic transformation. Lastly, although biomaterial scaffolds have facilitated axonal regrowth, these treatments do not restore the loss of neural cells and underlying circuitry that is the cause of the motor symptoms (Borisoff et al., 2003; Moore et al., 2006; Silva et al., 2010). Thus, there is currently no strategy that addresses both the loss of SNpc neurons and the dopaminergic axonal inputs into the striatum.

As a strategy to physically reconstruct lost long-distance axonal pathways in the brain, we are developing microtissue engineered neural networks (micro-TENNs), a novel class of transplantable, anatomically inspired three-dimensional (3D) cylindrical constructs composed of discrete neuronal population(s) spanned by internalized long-projecting axonal tracts (Cullen et al., 2012; Harris et al., 2016; Struzyna et al.,

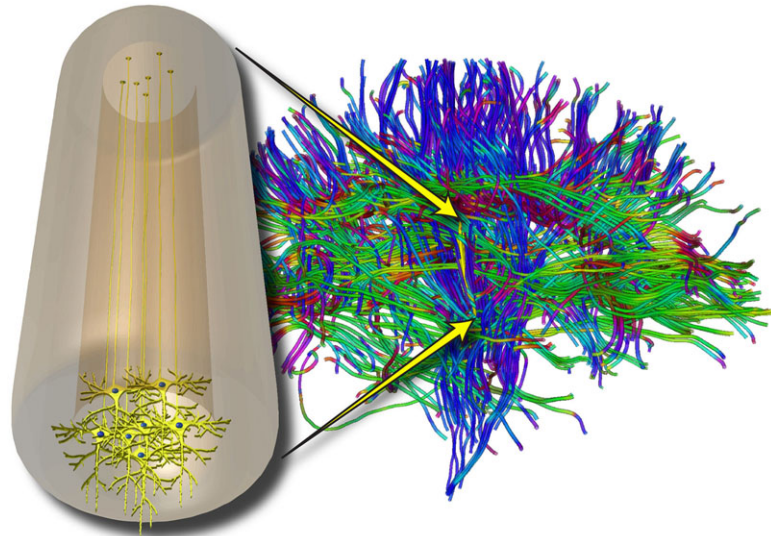
2015; Struzyna, Harris, Katiyar, Chen, & Cullen, 2015; Struzyna, Katiyar, & Cullen, 2014). Despite being only several hundred microns in diameter, micro-TENNs may feature axonal extension of at least several centimetres to reconstruct long-distance brain pathways lost due to trauma or neurodegenerative disease (Cullen et al., 2012; Harris et al., 2016; Struzyna et al., 2014; Struzyna, Harris, et al., 2015; Struzyna, Wolf, et al., 2015). We employ novel microtissue engineering techniques to create the neuronal-axonal constructs within a miniature tubular hydrogel featuring an interior extracellular matrix (ECM) core that supports neurite extension *in vitro*. The miniature form factor allows for minimally invasive delivery into the brain (Harris et al., 2016), whereas the biomaterial encasement protects the preformed cytoarchitecture and gradually degrades over several weeks (Struzyna, Wolf, et al., 2015). In rat models, we have previously demonstrated that allogeneic micro-TENNs composed of cerebral cortical neurons maintained their axonal architecture, and structurally integrated into the native nervous system (Struzyna, Wolf, et al., 2015).

In this study, we have significantly advanced this microtissue engineering approach by creating transplantable constructs that mimic the general cytoarchitecture of the nigrostriatal pathway. Specifically, we report the construction of the first micro-TENNs composed of a discrete population of dopaminergic neurons with long-projecting, unidirectional axonal tracts within transplantable miniature tubular hydrogels. We advanced our microfabrication techniques by seeding tubular microcolumns with engineered neuronal aggregates generated from primary embryonic rat dopaminergic neurons. We systematically varied ECM constituents, growth factors, and the presence of a neuronal target population in order to optimize the length of unidirectional axonal extension. *In vitro*, we confirmed that these micro-TENNs exhibited evoked dopamine release and found immunocytochemical evidence that they formed synapses with striatal neurons. Moreover, we stereotaxically implanted preformed dopaminergic micro-TENNs *en masse* to mimic the nigrostriatal pathway in rats, revealing construct neuronal survival and maintenance of axonal architecture to at least 1 month post implant. These microconstructs mimic the cytoarchitecture and functional characteristics of the nigrostriatal pathway, while providing the first evidence of dopaminergic axonal extension >6 mm and evoked dopamine release within implantable 3D constructs. We also showed proof-of-concept for clinical translation by generating micro-TENNs with dopaminergic neurons differentiated from human embryonic stem cells (hESCs), revealing at least several millimetres of unidirectional axonal extension within implantable hydrogel microcolumns. This novel strategy may uniquely address gaps in current Parkinson's disease treatments by allowing simultaneous replacement of dopaminergic neurons in the substantia nigra as well as their long-distance axonal projections to the striatum (Figure 1).

2 | MATERIALS AND METHODS

All procedures were approved by the IACUCs at the University of Pennsylvania and The Corporal Michael J. Crescenz Veterans Affairs Medical Center and were carried out in accordance with Public Health Service Policy on Humane Care and Use of Laboratory Animals (2015).

FIGURE 1 Reconstruction of the nigrostriatal pathway using microtissue engineered neural networks (micro-TENNs). A diffusion tensor imaging representation of the long-distance axonal tracts that connect discrete populations of neurons in the human brain. This conceptual rendition shows how a unidirectional micro-TENN—consisting of a population of dopaminergic neurons extending long, aligned processes—can be used to recreate the nigrostriatal pathway (yellow) that degenerates in Parkinson's disease. Axons in the substantia nigra are expected to functionally integrate with the transplanted dopaminergic neurons in the micro-TENN, whereas the transplanted dopaminergic axons are expected to functionally integrate with neurons in the striatum. After receiving appropriate inputs from the substantia nigra, the transplanted neurons will release dopamine in the striatum, thereby recreating the circuitry lost in Parkinson's disease [Colour figure can be viewed at wileyonlinelibrary.com]



2.1 | 3D micro-TENN fabrication

All supplies were from Invitrogen, BD Biosciences, or Sigma-Aldrich unless otherwise noted. Micro-TENNs were composed of an agarose (Sigma; A9539) ECM hydrogel moulded into a cylinder through which axons could grow. The outer hydrogel structure consisted of 1% agarose in Dulbecco's phosphate-buffered saline (DPBS). The agarose cylinder, with an outer diameter of 398 μm , was generated by drawing the agarose solution into a capillary tube (Drummond Scientific) via capillary action. An acupuncture needle (diameter: 160 μm ; Seirin) was inserted into the centre of the agarose-filled capillary tube in order to produce an inner column. Cured microcolumns were pushed out of the capillary tubes using a 30 gauge needle (BD; 305128) and placed in DPBS where they were cut to 6–12 mm in length and sterilized under UV light (1 hr). Five microlitres of the appropriate ECM cocktail was added to each microcolumn. ECM cocktails included rat tail Type 1 collagen, 1.0 mg/ml; rat tail Type I collagen, 1.0 mg/ml mixed with mouse laminin, 1.0 mg/ml; mouse laminin, 1.75 mg/ml; and rat tail Type 1 collagen, 1.0 mg/ml in 11.70 mM N-(3-Dimethylaminopropyl)-N'-ethylcarbodiimide hydrochloride, 4.3 mM N-Hydroxysuccinimide, and 35.6 mM sodium phosphate monobasic. These microcolumns were then incubated at 37 $^{\circ}\text{C}$ for 15–30 min, after which DPBS was added to the petri dish.

2.2 | Neuronal cell culture

Female Sprague-Dawley rats (Charles River) were the source for primary ventral mesencephalic neurons, a midbrain region previously shown to be enriched in dopaminergic neurons (Weinert, Selvakumar, Tierney, & Alavian, 2015). Carbon dioxide was used to euthanize timed-pregnant rats (embryonic Day 14), following which the uterus was extracted. The brains were removed in Hank's balanced salt solution (HBSS) and the ventral midbrain was isolated (Pruszek, Just,

Isacson, & Nikkhah, 2009). The ventral midbrains were dissociated in accutase for 10 min at 37 $^{\circ}\text{C}$. The cells were centrifuged at a relative centrifugal force of 200 for 5 min and resuspended at 1–2 million cells/ml in standard media consisting of Neurobasal medium + 2% B27 + 1% fetal bovine serum (Atlanta Biologicals) + 2.0 mM L-glutamine + 100 μM ascorbic acid + 4 ng/ml mouse basic fibroblast growth factor (bFGF) + 0.1% penicillin–streptomycin. High concentration growth media consisted of Neurobasal medium + 2% B27 + 1% fetal bovine serum (Atlanta Biologicals) + 2.0 mM L-glutamine + 100 μM ascorbic acid + 0.1% penicillin–streptomycin + 12 ng/ml mouse bFGF + 10 ng/ml brain-derived neurotrophic factor + 10 ng/ml glial cell-derived neurotrophic factor + 10 ng/ml ciliary neurotrophic factor + 10 ng/ml cardiotrophin. Dopaminergic neuron aggregates were created based on protocols adapted from Ungrin, Joshi, Nica, Bauwens, and Zandstra (2008). Custom-built arrays of inverted pyramidal wells were fabricated using polydimethylsiloxane (Sylgard 184, Dow Corning) cast from a 3D printed mould and placed in a 12-well plate. Twelve microlitres of the cell solution was transferred to each pyramidal well, and the 12-well plate was centrifuged at 1,500 rpm for 5 min, after which 2 ml of standard media was placed on top of each array. The centrifugation resulted in forced aggregation of neurons (approximately 3,200 cells per aggregate). The wells were then incubated overnight. At the time of plating, the DPBS was removed from the dishes containing the microcolumns and replaced with media. Using forceps, the aggregates were inserted into one (unidirectional) or both (bidirectional) ends of the microcolumns, and the cultures were placed in an incubator (total micro-TENNs created with primary dopaminergic neurons: $n = 310$).

H9 hESCs (passages 90–100, NIH code WA09; Wicell, Madison, WI, USA) were maintained on mouse embryonic fibroblast feeder cells (CF-1; MTI-Globalstem, Gaithersburg, MD, USA), and cultured in hESC media containing the following components: DMEM/F12 (Invitrogen, Carlsbad, CA, USA), 20% KnockOut serum replacement (Invitrogen),

1 mM non-essential amino acids (Invitrogen), 1X GlutaMax (Invitrogen), 0.1 mM β -mercaptoethanol (Sigma-Aldrich, St. Louis, MO, USA), 100 U/ml penicillin/100 μ g/ml streptomycin (Invitrogen), and 6 ng/ml bFGF (R&D Systems, Minneapolis, MN, USA). The stem cells were differentiated into dopaminergic neurons using the protocol outlined in Kriks et al. (2011). Differentiated dopaminergic neurons (Day 45) were then dissociated using accutase, after which aggregates were created and inserted into microcolumns as described above (total micro-TENNs created with differentiated dopaminergic neurons: $n = 5$). They were maintained in media consisting of Neurobasal medium + 2% B27 + 2.0 mM L-glutamine + 0.2 mM ascorbic acid + 20 ng/ml brain-derived neurotrophic factor + 20 ng/ml glial cell-derived neurotrophic factor + 1 ng/ml transforming growth factor β 3 + 0.5 mM dibutyl cAMP + 10 nM DAPT.

For micro-TENNs containing dissociated cells with no ECM core, dopaminergic cells were suspended in standard media at 10 million cells/ml and 5 μ l of this cell suspension was added to each microcolumn. The micro-TENNs were incubated for 60 min, after which media was added. For micro-TENNs containing dissociated cells with an ECM core, dopaminergic cells were suspended in rat tail Type 1 collagen, 1.0 mg/ml (10,000,000 cells/ml) at the time of plating and 5 μ l of this mixture was added to each microcolumn. The micro-TENNs were incubated for 15 min, after which media was added.

Prewarmed media was used to replace the culture media every 3–4 days *in vitro* (DIV). In some instances, micro-TENNs were transduced with an adeno-associated virus (AAV) vector (AAV2/1.hSynapsin. EGFP.WPRE.bGH, UPenn Vector Core) to express green fluorescent protein (GFP) in the neurons. Here, at 3 DIV, the micro-TENNs were incubated overnight in media containing the vector (3.2×10^{10} genome copies/ml) and the cultures were rinsed with media the following day.

Female Sprague-Dawley rats (Charles River, Wilmington, MA, USA) were the source for primary striatal neurons. Carbon dioxide was used to euthanize timed-pregnant rats (embryonic Day 18), after which the uterus was extracted. To isolate striatal neurons, the brains were removed in HBSS and striata were isolated. The striata were dissociated in trypsin (0.25%) + ethylenediaminetetraacetic acid (EDTA; 1 mM) for 12 min at 37 °C. The trypsin-EDTA was then removed and the tissue was triturated in HBSS containing DNase I (0.15 mg/ml). The cells were centrifuged at 1,000 rpm for 3 min and resuspended at 1–2 million cells/ml in Neurobasal medium + 2% B27 + 0.4 mM L-glutamine. Striatal aggregates were created and inserted into micro-TENNs as previously described. When testing if dopaminergic aggregates would form synapses with striatal aggregates, striatal aggregates were inserted into the vacant ends of dopaminergic micro-TENNs at 10 DIV. When testing if striatal aggregates would increase the growth rate of dopaminergic micro-TENNs, they were inserted at 3 DIV.

2.3 | Immunocytochemistry

Micro-TENNs were fixed in 4% formaldehyde for 35 min and permeabilized using 0.3% Triton X100 plus 4% horse serum for 60 min. Primary antibodies were added (in phosphate-buffered saline (PBS) + 4% serum) at 4 °C for 12 hr. The primary antibodies were the following markers: (a) β -tubulin III (1:500, Sigma-Aldrich, cat # T8578), a microtubule element expressed primarily in neurons; (b) tyrosine hydroxylase

(TH; 1:500, Abcam, cat # AB113), an enzyme involved in the production of dopamine; (c) microtubule-associated protein 2 (1:500, Millipore, cat # AB5622), a microtubule-associated protein found in neuronal somata and dendrites; (d) dopamine-and-cAMP-regulated neuronal phosphoprotein (DARPP-32; 1:250, Abcam, cat # AB40801), a protein found in striatal medium-sized spiny neurons; and (e) Synapsin 1 (1:1000, Synaptic Systems, cat # 106001), a protein expressed in synaptic terminals of the central nervous system. Appropriate fluorescent secondary antibodies (Alexa-488, -594, and/or -649 at 1:500 in PBS + 30 nM Hoechst + 4% serum) were added at 18–24 °C for 2 hr.

2.4 | Fast scan cyclic voltammetry

Micro-TENNs were fabricated for these studies as described above but using a larger diameter (500 μ m ID, 973 μ m OD) to allow for greater DA signal. At 24 DIV, micro-TENNs were transferred to a testing chamber and flushed with culture media containing 100 μ M L-DOPA. A carbon fibre electrode (150–200 μ m length \times 7 μ m diameter) was inserted either into the dopaminergic aggregate ($n = 3$) or at the axon terminals ($n = 1$), and a bipolar stimulating electrode (Plastics One, Roanoke, VA, USA) was placed across the aggregate. Dopamine release was elicited using electrical pulse trains (30 Hz, 5 ms pulse width, 1 s, monophasic) every 5 min and recorded using Demon Voltammetry and Analysis Software (Yorgason, España, & Jones, 2011). The potential of the carbon fibre electrode was linearly scanned from -0.4 to 1.2 V and back to -0.4 V versus Ag/AgCl. A voltmeter/amperometer (Chem-Clamp; Dagan Corporation) was used to scan at a rate of 400 V/s, and cyclic voltammograms were recorded every 100 ms. Electrode calibrations of known concentrations of DA (1–10 μ M) were used to calculate the concentration of electrically evoked dopamine release at the peak oxidation potential for dopamine in consecutive voltammograms.

2.5 | Transplantation of micro-TENNs

Male Sprague-Dawley rats (325–350 g) were anesthetized with isoflurane and mounted in a stereotactic frame. The scalp was cleaned with betadine, bupivacaine was injected along the incision line, and a midline incision was made to expose Bregma. A 5 mm craniectomy was centered at the following coordinates in relation to Bregma: +4.8 mm (AP), 2.3 mm (ML). The micro-TENN was loaded into a needle (OD: 534 μ m, ID: 420 μ m; Vita Needle, Needham, MA, USA) attached to a Hamilton syringe mounted on a stereotactic arm. The stereotactic arm was positioned at 34° relative to the horizontal plane, the dura was opened, and the needle lowered into the brain to a depth of 11.2 mm. The needle was kept in place for 10 s, at which time a stationary arm was positioned to contact the plunger of the Hamilton syringe to ensure that the micro-TENN was expelled. The needle containing the micro-TENN was then withdrawn from the brain. The scalp was sutured closed and buprenorphine was provided for postoperative analgesia. Animals receiving micro-TENNs were survived for 15 min, ($n = 5$), 1 week ($n = 5$), or 1 month ($n = 5$). At the time of sacrifice, animals were anesthetized and underwent transcardial perfusion with heparinized saline followed by 10% formalin.

2.6 | Immunohistochemistry

After 24 hr postfix in 4% paraformaldehyde, brains were prepared for optical clearing, paraffin processing, or cryosectioning.

For optical clearing, Visikol Inc.'s histology protocol was followed (Merz, Schwenk, Shah, Necaise, & Salafia, 2017). Briefly, brains were cut into 1 mm sections using a vibratome, dehydrated in a series of methanol washes, treated with hydrogen peroxide, and then rehydrated. Sections were permeabilized in a buffer containing PBS, 0.2% Triton X-100, 0.3 M glycine, and 20% DMSO. Sections were blocked with 6% horse serum for 3 days, and then incubated in primary antibodies (Sheep anti-TH, 1:100, Abcam, cat #ab113; Rabbit anti-NeuN, 1:100, cat #abn78) for 3 days. Next, they were incubated in secondary antibodies (1:250) for 3 days. They were then dehydrated, treated with Visikol® HISTO-1™ for 18 hr, and imaged in Visikol® HISTO-2™.

For paraffin processing, brains were blocked sagittally, processed through paraffin, cut at 8 μm , mounted on slides, and processed for immunohistochemistry. Paraffin sections were deparaffinized and then rehydrated. Endogenous peroxidase was quenched using 3% hydrogen peroxide in water (Fisher, cat #S25359), followed by heat-induced epitope retrieval in TRIS-EDTA. Sections were blocked with horse serum (ABC Universal Kit, Vector Labs, cat #PK-6200) for 30 min. Rabbit anti-TH (1:750; Abcam, cat #ab112) was applied in Optimax buffer overnight at 4 °C. The antigen of interest was visualized using DAB (Vector Labs, cat # SK-4100).

For cryosectioning, brains were blocked sagittally, put into 30% sucrose until saturated, and then frozen. Sections were cryosectioned at 35 μm , mounted on slides, and processed for immunohistochemistry. Frozen sections were blocked with 5% normal horse serum in 0.1% Triton-x/PBS for 30–45 min. Primary antibodies (Rabbit anti-TH, 1:750, Abcam AB112; Mouse anti-Tuj1, 1:1000, Sigma T8578) were applied to the sections in 2% horse serum/Optimax buffer for 2 hr at room temperature. Secondary antibodies (1:1000) were applied in 2% horse serum/PBS for 1 hour at room temperature. Sections were counterstained with Hoechst.

2.7 | Microscopy and data acquisition

For *in vitro* analyses, micro-TENNs were imaged using phase-contrast and fluorescence on a Nikon Eclipse Ti-S microscope with image acquisition using a QiClick camera interfaced with Nikon Elements. In order to determine the length of neurite penetration, the longest observable neurite in each micro-TENN was measured from the proximal end of the neuronal aggregate after fixation. For *in vitro* immunocytochemistry analyses, cultures and micro-TENNs were fluorescently imaged using a Nikon A1RSI Laser Scanning Confocal microscope. All micro-TENN confocal reconstructions were from full thickness z-stacks. For analysis of micro-TENNs posttransplant into the brain, micro-TENNs were fluorescently imaged using a Nikon A1RSI Laser Scanning Confocal microscope. Each section was analysed to assess the presence, architecture, and outgrowth/integration of micro-TENN neurons/neurites.

2.8 | Statistical analyses

No method was used to predetermine the sample sizes of groups. Due to obvious visual differences between experimental groups (e.g.,

dissociated vs. aggregate neuron micro-TENNs), in many cases, it was not possible for investigators to be blinded to treatment group during experiments or data assessment. For *in vivo* transplant studies, rats were randomly assigned for use in this experiment. The normality of all data was examined, and adjustments were made for non-normal data. An unpaired, parametric two-sided *t*-test was performed to determine if there were statistically significant differences in axonal outgrowth between unidirectional versus bidirectional micro-TENNs containing a dopaminergic end target. Unpaired, nonparametric, two sided Mann–Whitney tests were performed to determine if there were statistically significant differences in axonal outgrowth between the following treatment pairs: dissociated versus aggregated cells, high versus regular growth factor concentration, and unidirectional versus bidirectional micro-TENNs containing a striatal end target. An unpaired, nonparametric, two sided Mann–Whitney test was performed to determine if there were statistically significant differences between the lengths of TH+ axons as a percentage of total axonal length with collagen I versus collagen I-laminin cocktail inner cores. ANOVA was performed for the ECM studies. When differences existed between groups, post hoc Tukey's pair-wise comparisons were performed. For all statistical tests, $p < .05$ was required for significance. Data are presented as mean \pm standard deviation.

3 | RESULTS

3.1 | Micro-TENNs plated with dissociated neuronal suspensions

Dopaminergic neurons were isolated from the ventral mesencephalon of embryonic rats. In planar culture, these neurons demonstrated a healthy neuronal morphology, the presence of dopaminergic neurons (based on TH expression), significant neurite outgrowth (based on β -tubulin III expression), and network formation out to 28 DIV (Figure S1A–C). To create dopaminergic micro-TENNs, we initially seeded microcolumns using dissociated neuronal suspensions. These dissociated cells infiltrated the length of the inner lumen and generally did not produce the desired cytoarchitecture of a discrete cell body region projecting axons across the length of the inner core (Figure S1D–H). However, the dissociated neurons within the microtissue constructs presented a healthy morphology, and occasionally, self-organized into the desired cytoarchitecture by chance (Figure S2). In these cases, unidirectional axonal projections achieved lengths of several millimetres, and, importantly, the health of these constructs was also maintained out to 28 DIV (Figure S2). In order to see if the inclusion of additional ECM in the inner core increased the consistency with which the correct architecture was generated, we suspended dissociated cells into collagen, and injected the mixture to gel inside the microcolumns. Unfortunately, the presence of the collagen did not aid in producing the desired cytoarchitecture, and the dissociated cells continued to spread throughout the length of the inner core (Figure 2a1–a3). Although these results demonstrated our ability to culture dopaminergic neurons that formed extensive neurite networks within hydrogel microcolumns, these techniques were not sufficient to consistently generate our desired cytoarchitecture.

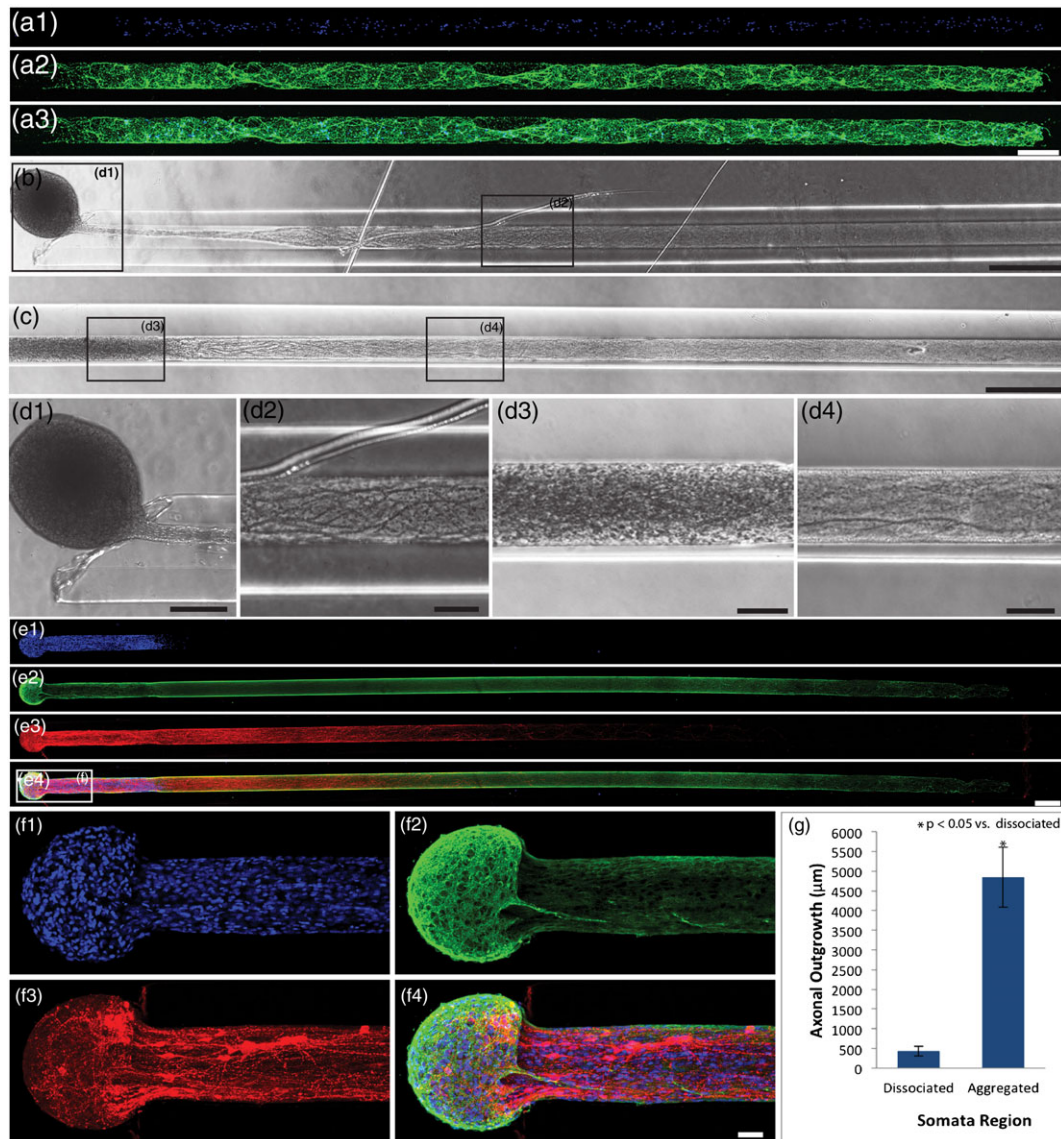


FIGURE 2 Improved microtissue engineered neural network (micro-TENN) cytoarchitecture using forced aggregation method. Phase contrast and confocal reconstructions of micro-TENNs plated with primary dopaminergic neurons at 14 days *in vitro*. (a) Representative micro-TENN plated with dissociated neurons labelled via immunocytochemistry to denote neurons/axons (β -tubulin III; green) and cell nuclei (Hoechst; blue). Dissociated micro-TENNs did not demonstrate the desired cytoarchitecture as they showed cell infiltration throughout the entire length of the inner core. (b,c) Phase contrast images depicting micro-TENNs plated with engineered dopaminergic neuron aggregates. Based upon plating technique, aggregates either (b) attached directly outside the agarose microcolumn or (c) inside the inner core. Higher magnification images from demonstrative regions in (b,c) show that although the (d1,d3) cell body regions differed between the two aggregate plating techniques, their (d2, d4) axonal regions were similar. (e) Representative aggregate micro-TENN labelled via immunocytochemistry to denote all neurons/axons (β -tubulin III; green) and dopaminergic neurons/axons (TH; red), with cell nuclei counterstain (Hoechst; blue). Aggregate micro-TENNs demonstrated the ideal cytoarchitecture, with (e1) discrete cell body regions and (e2,e3) axonal regions. (f) A higher magnification reconstruction from a demonstrative region in (e) depicts the aggregated cell bodies. (g) Micro-TENNs generated using aggregates demonstrated a greater extent of axonal outgrowth than micro-TENNs plated with dissociated neurons ($n = 13$ micro-TENNs each group; Mann-Whitney test, $p < .0001$). Data are presented as mean \pm standard deviation. Scale bar (a) = 250 μm . Scale bar (b,c) = 500 μm . Scale bar (d1) = 200 μm . Scale bar (d2-d4) = 100 μm . Scale bar (e) = 250 μm . Scale bar (f) = 50 μm [Colour figure can be viewed at wileyonlinelibrary.com]

3.2 | Forced neuronal aggregation method

As our previous micro-TENN fabrication methods did not reliably generate the desired cytoarchitecture, we adapted a method to mechanically group cells into aggregates (Ungrin et al., 2008). After dissociating embryonic tissue into a single cell suspension, this solution was centrifuged in inverted pyramidal wells in order to pellet the neurons at the bottom of the wells. The wells were left in the incubator overnight,

during which the pelleted cells became aggregated spheres of neurons (Figure S3). Once formed, the aggregates were inserted into the ends of the agarose microcolumns. This method consistently produced micro-TENNs with distinct cell body and axonal regions. Furthermore, we found that based upon the depth and placement of the aggregate within the microcolumn, we could create micro-TENNs that exhibited either an externalized or internalized cell body region (Figure 2b-d). Moreover, this technique produced long-projecting unidirectional

axonal tracts, as demonstrated based on TH and β -tubulin III immunoreactivity (Figure 2e–f). Indeed, as measured by the length of the longest neurite in each micro-TENN, it was determined that the axons projecting from the aggregates grew approximately 10 \times longer than analogous axons extending within microcolumns seeded with dissociated neurons (Figure 2g).

3.3 | Optimization of micro-TENN length

Once we were able to consistently produce micro-TENNs with the desired cytoarchitecture, we optimized microcolumn features and environmental conditions to produce micro-TENNs with the longest possible axonal outgrowth. As the nigrostriatal pathway measures approximately 6 mm in the rat, we attempted to generate micro-TENNs at least 6 mm in length. Here, we tested the effects of the ECM constituents in the inner lumen, presence of growth factors, and the micro-TENN directionality on outgrowth. It was found that collagen I and collagen I + laminin resulted in the longest axonal outgrowth, as measured by the length of the longest neurite in each micro-TENN at 14 DIV (Figure 3). The average axonal outgrowth for the collagen I and collagen I + laminin cores was $4,892 \pm 703$ and

$4,686 \pm 921 \mu\text{m}$, respectively. In contrast, it was found that crosslinked collagen ($1,227 \pm 481 \mu\text{m}$), laminin-coated ($205 \pm 615 \mu\text{m}$), and empty cores ($\sim 0 \mu\text{m}$) resulted in significantly reduced neurite outgrowth. For the two highest performing groups (lumen composed of collagen or collagen + laminin), it was determined that TH⁺ dopaminergic axonal projections attained at least 60% of the maximal axonal length (Figure 3f).

We also tested the effect of the media growth factor concentration on axonal outgrowth within the microcolumns. A media containing a relatively low concentration of bFGF (4 ng/ml) was compared with media containing high concentrations of growth factors previously shown to increase dopaminergic neuron outgrowth and survival (Hyman et al., 1991). At 14 DIV, we found that the high growth factor concentration media did not result in denser or longer axonal outgrowth compared with the low concentration media ($n = 14$ micro-TENNs in each group; Figure S4). Lastly, we investigated whether the use of a target population of dopaminergic cells would increase axonal outgrowth. Bidirectional dopaminergic micro-TENNs were plated by inserting dopaminergic aggregates into both ends of the microcolumns. Because the two dopaminergic neuron populations were separated by 1.2 cm, we sought to assess whether chemotactic

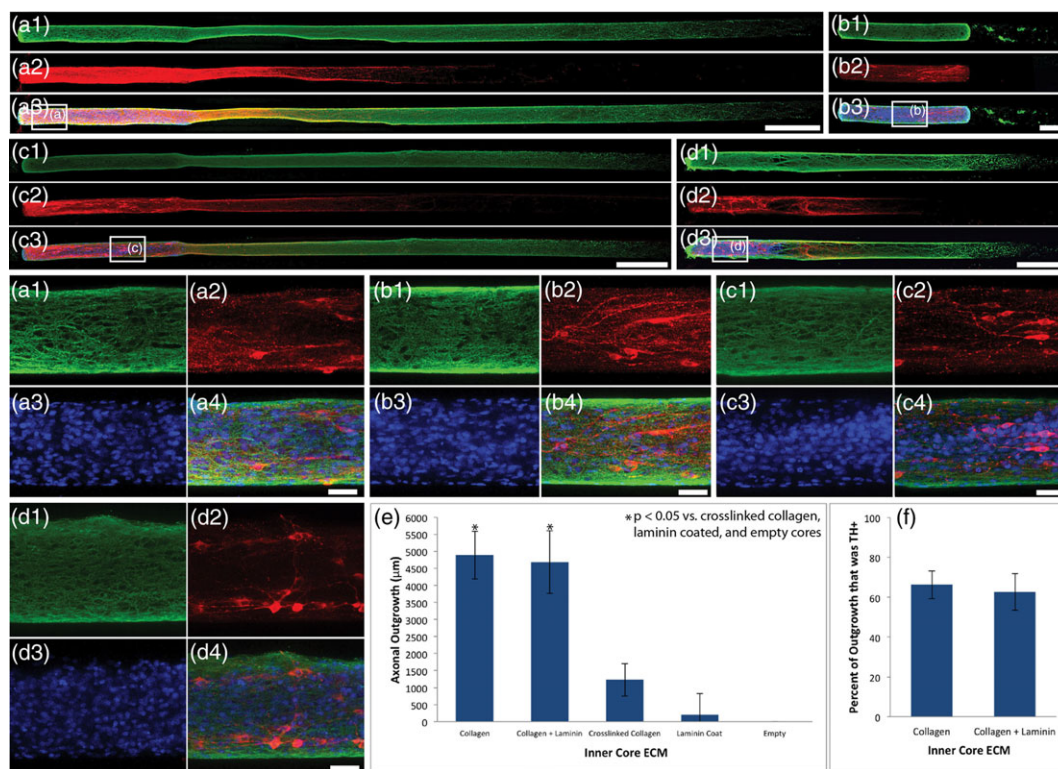


FIGURE 3 Effect of extracellular matrix (ECM) on axonal outgrowth within microtissue engineered neural networks (micro-TENNs). Representative confocal reconstructions of dopaminergic micro-TENNs plated with different ECM cores. At 14 days *in vitro*, all micro-TENNs were labelled via immunocytochemistry to denote all neurons/axons (β -tubulin III; green) and dopaminergic neurons/axons (TH; red), with nuclear counterstain (Hoechst; blue). The type of ECM strongly influenced axonal outgrowth, with (a) collagen I ($n = 12$ micro-TENNs) and (c) collagen I + laminin cocktail ($n = 12$) supporting the longest axonal outgrowth. Micro-TENNs with (b) empty cores ($n = 9$) or (d) crosslinked collagen cores ($n = 11$) demonstrated significantly less outgrowth. (a–d) Higher magnification reconstructions from demonstrative regions in (a–d) show similar expression of TH across groups. (e) A one way ANOVA ($p < .0001$) followed by a post hoc Tukey’s test determined that collagen I and collagen I-laminin cocktail cores were statistically equal ($p = .8590$), and that they each supported axonal outgrowth that was statistically longer than outgrowth in empty ($p < .0001$), laminin-coated ($p < .0001$), or crosslinked collagen ($p < .0001$) cores (* denotes significance). (f) As determined by a Mann–Whitney test, the lengths of TH⁺ axons as a percentage of total axonal length were statistically equivalent between the collagen I ($n = 12$) and collagen I + laminin ($n = 12$) inner cores ($p = .9723$). Data are presented as mean \pm standard deviation. Scale bar (a,c,d) = 500 μm . Scale Bar (b) = 250 μm . Scale bar (e–h) = 50 μm [Colour figure can be viewed at wileyonlinelibrary.com]

signalling between the populations would increase outgrowth. However, at 14 DIV, we determined that the axonal outgrowth in bidirectional micro-TENNs was not greater than axonal outgrowth in unidirectional micro-TENNs ($n = 14$ micro-TENNs in each group; Figure S4).

Overall, we found that the use of engineered neuronal aggregates and specific ECM constituents were critical factors in axonal extension, whereas high growth factor media and the presence of a target neuron population did not affect axonal outgrowth. Of note, the mean neuronal aggregate length at 14 DIV was $1,165 \pm 212 \mu\text{m}$; therefore, the total micro-TENN length (neuronal aggregate + axon length) attained using dopaminergic aggregates in collagen was >6 mm by 14 DIV—suitable to span the nigrostriatal pathway in rats.

Following these optimization studies, we fabricated dopaminergic micro-TENNs with an inner core of collagen I and allowed them to grow over 28 DIV to ascertain if axonal extension progressed further within the microcolumns. We found continued axonal extension out to 28 DIV, with lengths of $6,046 \pm 670 \mu\text{m}$ for dopaminergic axons, $7,697 \pm 1,085 \mu\text{m}$ for all axons, and $8,914 \pm 1,187 \mu\text{m}$ for total aggregate + axon lengths. In some cases, maximum total micro-TENN lengths at this time point were over 10 mm, well beyond what would be required to span the nigrostriatal pathway in rats (Figure 4).

3.4 | Dopamine release *in vitro*

Fast scan cyclic voltammetry (FSCV) was used to examine the capacity of the micro-TENNs to release dopamine *in vitro*. At 24 DIV, a carbon fibre electrode was used to record evoked dopamine release in both the dopaminergic aggregate and at the distal end of the microcolumn containing the terminals of the axonal tracts. Following incubation in media containing L-DOPA, it was found that dopamine release could be elicited in both the somatic and axonal regions (Figure 5). Cyclic voltammograms recorded during dopamine release in the neuronal aggregate region all demonstrated characteristic oxidation between 0.55 and 0.65 V, and reduction between -0.20 and -0.30 V (Heien, Phillips, Stuber, et al., 2003). Under the parameters used in these studies, the pattern of oxidation and reduction may be used to correctly identify currents produced by action potential dependent release of catecholamines. Current traces recorded in the aggregate region across several micro-TENNs demonstrated an average peak extracellular dopamine concentration of ~ 30 nM immediately following electrical stimulation (Figure 5). Of note, this protocol was also applied to multiple micro-TENNs at 9 DIV but measurements of evoked dopamine release were not attained (data not shown), suggesting the need for functional maturation of dopaminergic neurons/axons over 24 DIV.

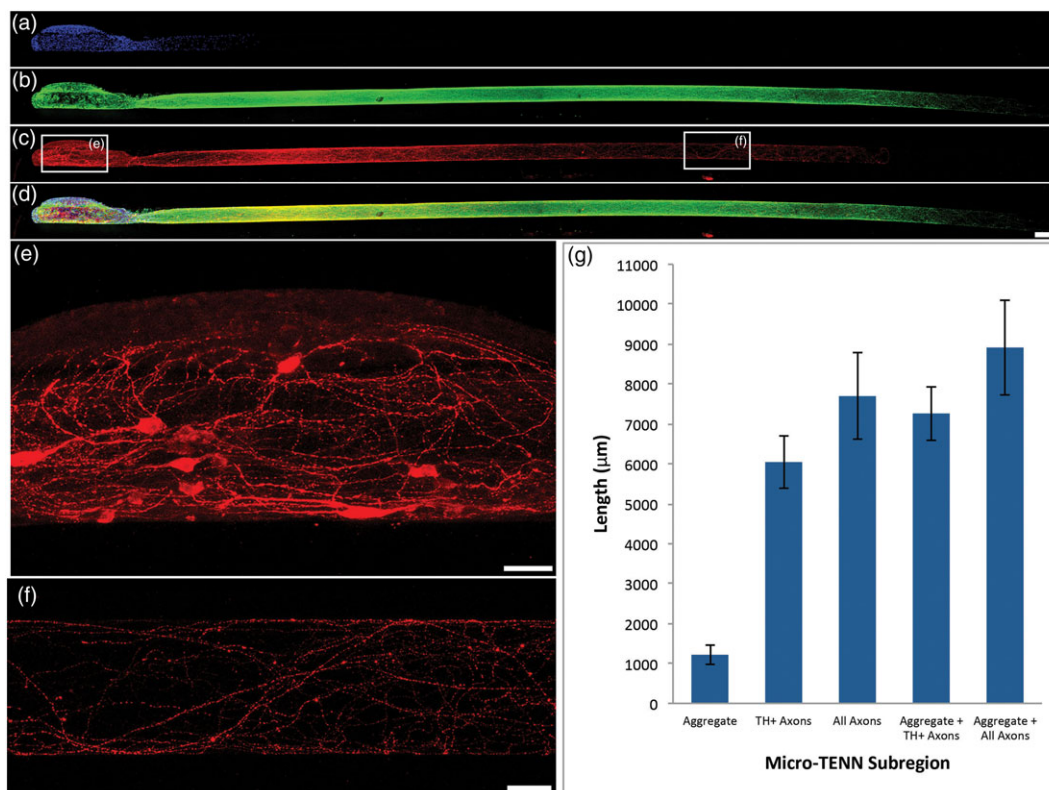


FIGURE 4 Long-projecting dopaminergic microtissue engineered neural networks (micro-TENNs). (a–f) Confocal reconstructions of a representative micro-TENN plated with a dopaminergic aggregate and collagen I inner core at 28 days *in vitro* (DIV). Micro-TENN labelled via immunocytochemistry to denote all neurons/axons (β -tubulin III; green) and dopaminergic neurons/axons (TH; red), with nuclear counterstain (Hoechst; blue). (a–d) Long-term dopaminergic micro-TENNs showed robust survival and axonal extension over 28 DIV. (e, f) Higher magnification reconstructions from demonstrative regions in (c) show healthy TH+ neurons and axons, with apparent axonal varicosities suggesting sites of dopamine release. (g) Micro-TENN length measurements taken at 28 DIV ($n = 7$ micro-TENNs) demonstrated TH+ axons measuring $6,046 \pm 670 \mu\text{m}$, and a total TH+ length of $7,264 \pm 672 \mu\text{m}$ with the inclusion of the dopaminergic aggregate. Importantly, these lengths are more than sufficient to span the nigrostriatal pathway in rats. Data are presented as mean \pm standard deviation. Scale bar (a–d) = $250 \mu\text{m}$. Scale bar (e, f) = $50 \mu\text{m}$ [Colour figure can be viewed at wileyonlinelibrary.com]

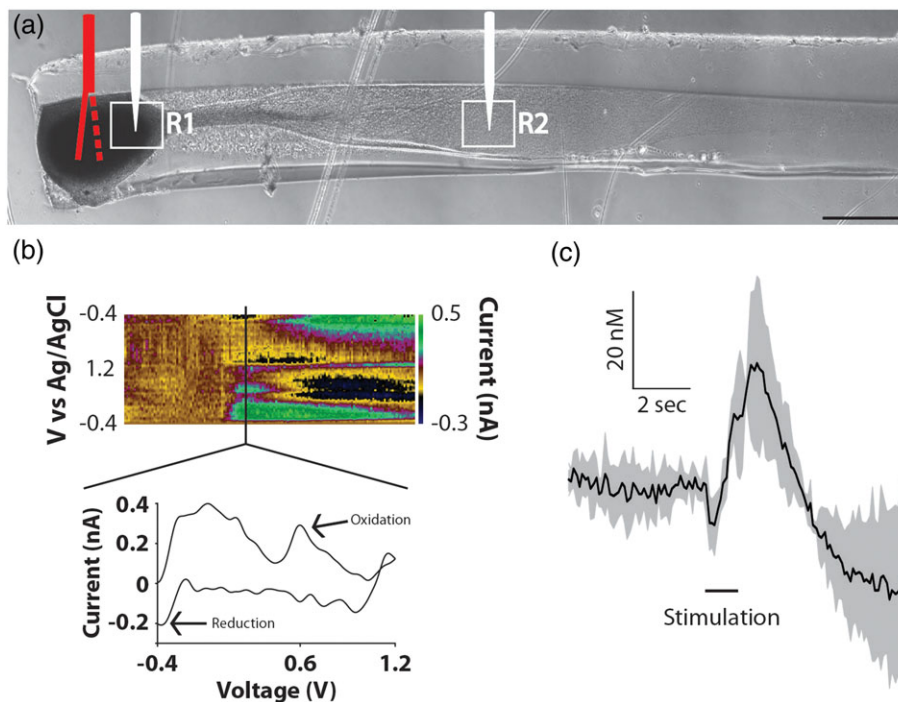


FIGURE 5 Evoked dopamine release from microtissue engineered neural networks (micro-TENNs) *in vitro*. (a) Recording set up for FSCV *in vitro*. A bipolar stimulating electrode (red) was placed to span the dopaminergic aggregate in the microcolumn, and was used to evoke dopamine release. A carbon fibre electrode (white) was used to record dopamine release either within the dopaminergic aggregate (R1) or at the axon terminals (R2). (b) Representative colour plot displaying the current recorded as the potential of the carbon fibre electrode was linearly scanned from -0.4 to 1.2 V and back to -0.4 V versus Ag/AgCl every 100 ms. The magnified cross section from the colour plot displays an individual cyclic voltammogram exhibiting an oxidation peak at 0.65 V and a reduction trough at -0.3 V, which are characteristic of dopamine. (c) The averaged concentration of dopamine released in the dopaminergic aggregate (R1) following electrical stimulation. Scale bar A = $500 \mu\text{m}$ [Colour figure can be viewed at wileyonlinelibrary.com]

3.5 | Formation of synapses with striatal population

As the dopaminergic axons comprising the nigrostriatal pathway synapse with striatal neurons in the brain, we probed the ability of our tissue engineered nigrostriatal pathway to synapse with a population of striatal neurons *in vitro*. Dopaminergic micro-TENNs were generated and, after 10 DIV, embryonic rat striatal aggregates were inserted into the vacant ends of the microcolumns. After 4 more DIV, immunocytochemistry was performed in order to assess potential synaptic integration between the two populations. This analysis confirmed the presence of the appropriate neuronal subtypes in the two aggregate populations, specifically, TH⁺ dopaminergic neurons and DARPP-32⁺ medium spiny striatal neurons (Figure 6). Moreover, confocal microscopy revealed extensive axonal–dendritic integration and putative synapse formation involving the dopaminergic axons and striatal neurons (Figure 6d,e,g,h). Also, immunocytochemistry confirmed that the majority of the striatal (DARPP-32⁺) neurites were also microtubule-associated protein 2⁺, suggesting that these were dendrites (data not shown). In order to determine if chemotactic cues generated by the striatal population influenced axonal outgrowth from the dopaminergic neuron aggregates, the length of axonal outgrowth was quantified with and without the striatal end target. It was found that the axonal outgrowth in dopaminergic micro-TENNs containing a target population of striatal neurons was not statistically greater than axonal outgrowth in unidirectional dopaminergic micro-TENNs ($n = 9$ micro-TENNs in each group; Figure 6f).

3.6 | Transplant and survival of preformed dopaminergic micro-TENNs *in vivo*

We sought to demonstrate the ability to precisely deliver preformed dopaminergic micro-TENNs into the brain as well as their survival and architecture at various time points post implant. Accordingly, dopaminergic aggregate micro-TENNs with an inner lumen containing collagen I (in some instances transduced to express GFP) were grown for 14 DIV, after which time they were drawn into a custom needle and stereotactically microinjected to approximate the nigrostriatal pathway in adult male Sprague-Dawley rats (Figure 7a,b). Animals were sacrificed either after 15 min or at 1 week and 1 month time points ($n = 5$ each). The tissue of animals that were sacrificed after 15 min was cleared and labelled with the dopaminergic marker TH in order to confirm that the transplantation process itself did not harm the micro-TENN cytoarchitecture, revealing surviving construct neurons in the substantia nigra and maintenance of their axonal projections within the microcolumn towards the striatum (Figure 7c,d). At 1 week and 1 month time points, surviving GFP⁺ neurons and axons were found within the micro-TENN lumen, which were easily identified spanning the nigrostriatal pathway because the agarose microcolumn had only partially degraded at these time points (Figure 7e,f). Histological sections were colabelled for the axonal marker β -tubulin III and the dopaminergic marker TH, revealing the preservation of a robust neuronal and dopaminergic axonal population. In particular, longitudinally projecting TH⁺ axons were present,

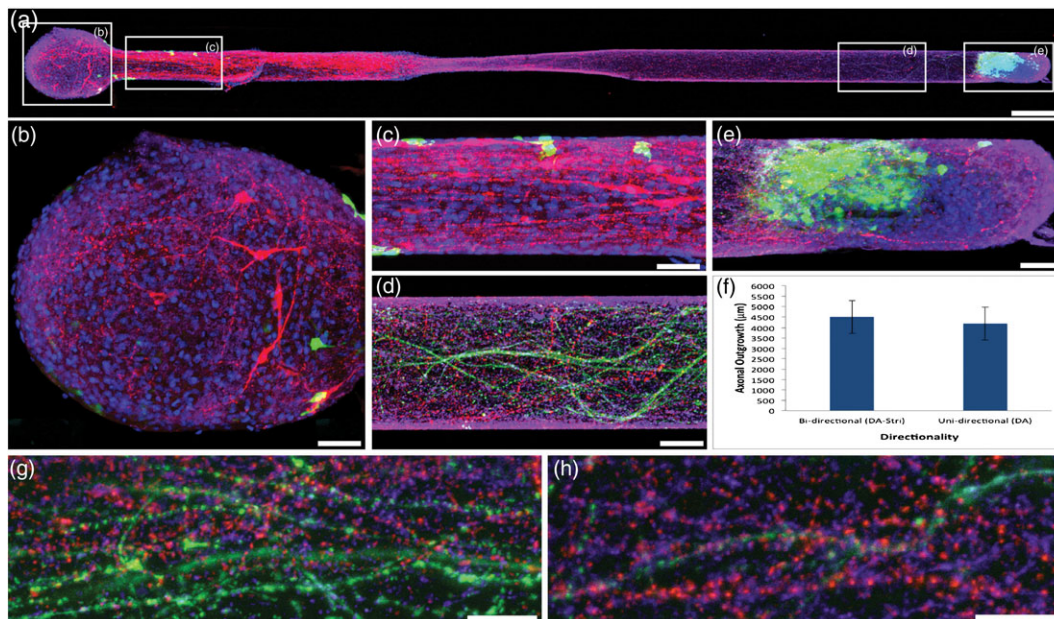


FIGURE 6 Synapse formation between microtissue engineered neural network (micro-TENN) dopaminergic axons and striatal neurons *in vitro*. (a) Representative confocal reconstruction at 14 days *in vitro* of a dopaminergic micro-TENN plated with an aggregated striatal end target. The micro-TENN was labelled via immunocytochemistry to denote dopaminergic neurons/axons (TH; pink), striatal (medium spiny) neurons (DARPP-32; green), and synapses (synapsin; purple), with nuclear counterstain (Hoechst; blue). (b–e) Higher magnification reconstructions from demonstrative regions in (a) depict the (b) dopaminergic neuron aggregate, (c) robust, aligned TH+ axons, and (d) neurite outgrowth from the striatal neuron population. (e) A high degree of synapsin labelling (purple) along the trajectory of TH+ axons (pink) suggests that dopaminergic axons formed synapses with the striatal neurons. (f) Micro-TENNs containing striatal end targets did not result in statistically longer axonal outgrowth when compared with unidirectional dopaminergic micro-TENNs with no end target ($n = 9$ micro-TENNs each group; Mann–Whitney test, $p = .9182$). Data are presented as mean \pm standard deviation. (g,h) Synapsin+ puncta (purple) can be seen decorating putative dendrites projecting from striatal neurons (green) shown with dopaminergic axonal varicosities (pink), further suggesting synaptic integration. Scale bar (a) = 250 μm . Scale bar (b–e) = 50 μm . Scale bar (g,h) = 20 μm [Colour figure can be viewed at wileyonlinelibrary.com]

which confirmed that the micro-TENNs were generally able to maintain their cytoarchitecture following longer-term transplantation into the brain.

3.7 | Generation of hESC-derived dopaminergic micro-TENNs

As our eventual goal is to enable translation of this strategy, we sought to assess the feasibility of generating micro-TENNs with dopaminergic neurons derived from human sources. As such, we assessed the ability to fabricate micro-TENNs with dopaminergic neurons differentiated from hESCs. The hESCs were differentiated following the protocol outlined in Kriks et al. (2011), after which they were lifted from 2D culture (Figure 8a), aggregated, and inserted into the microcolumns. At 14 days following plating in the microcolumns, it was found that these micro-TENNs displayed the correct cytoarchitecture of a discrete somatic zone with unidirectional axonal tracts within the lumen of the hydrogel microcolumn. These axonal extensions measured over 4 mm in length at this time point (Figure 8b). These human dopaminergic micro-TENNs colabelled for the axonal marker β -tubulin III and the dopaminergic marker TH, and showed a purity of roughly 50% dopaminergic neurons (data not shown).

4 | DISCUSSION

Current treatments for Parkinson's disease, including the use of dopamine replacement strategies and DBS, are aimed at alleviating motor disabilities rather than correcting the underlying cause of the motor symptoms. Furthermore, although dopaminergic neuron and/or fetal graft implants into the striatum may provide a local source of dopamine, these approaches do not recreate the nigrostriatal circuit and thus do not provide appropriate feedback control of dopamine release. To address these gaps, we sought to develop a tissue-engineered solution that could be precisely delivered to physically restore lost dopaminergic neurons in the SNpc and their axonal projections to the striatum. To achieve this objective, we built upon our lab's previously developed microtissue engineering platform by generating the first micro-TENNs utilizing primary dopaminergic neurons. It was found that micro-TENNs plated with neuronal aggregates grew more than 6 mm in length when fabricated with the optimal inner core ECM. Furthermore, the dopaminergic micro-TENNs exhibited evoked dopamine release and were capable of synapsing with a population of striatal cells *in vitro*, and showed survival and maintenance of cytoarchitecture upon transplant *in vivo*.

Dopaminergic micro-TENNs were fabricated using a population of ventral mesencephalic neurons that, although enriched in dopaminergic neurons, are not a pure dopaminergic population. The impurity of the population may or may not matter functionally following

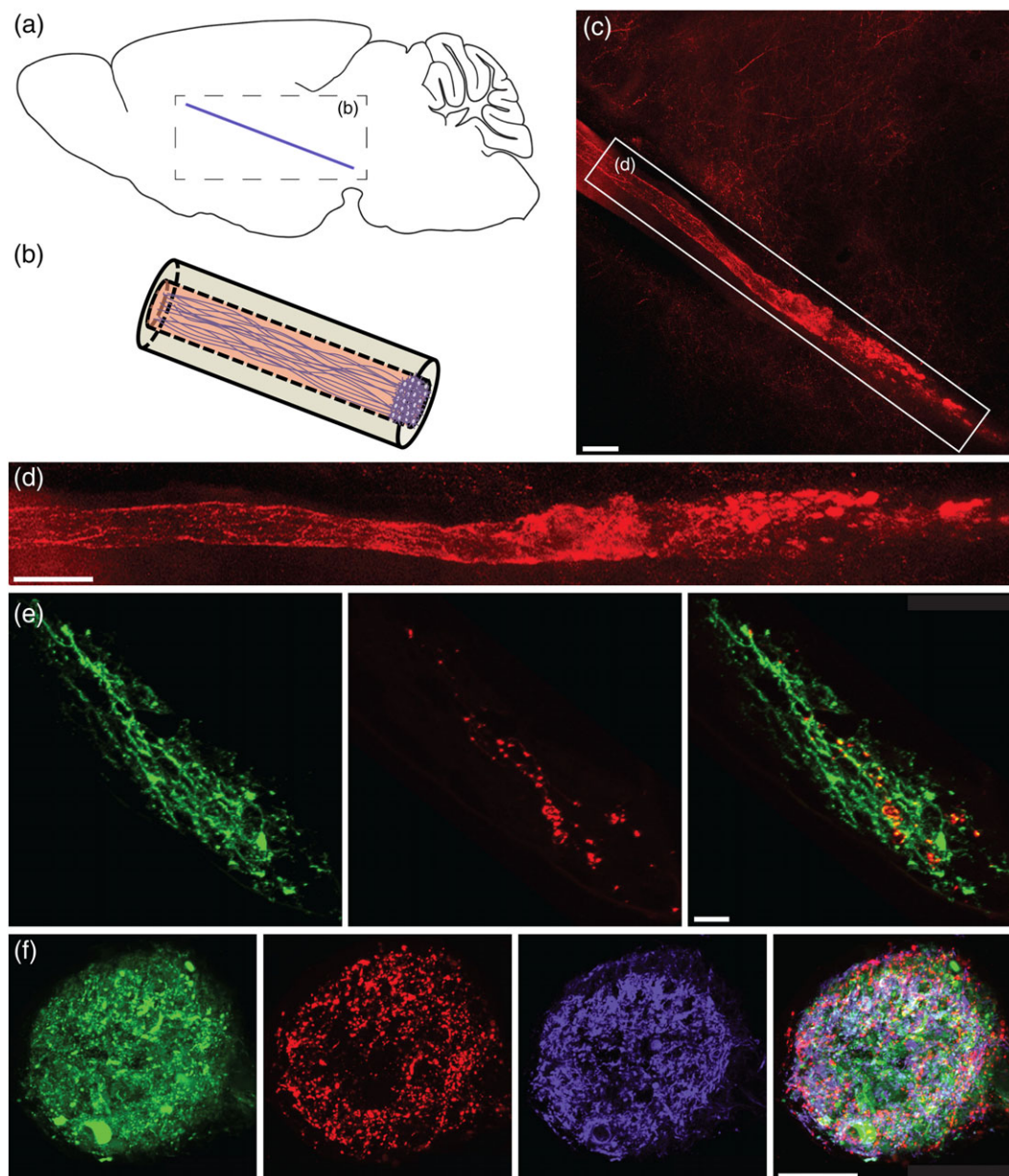


FIGURE 7 Microtissue engineered neural network (micro-TENN) neuronal survival and maintenance of axonal cytoarchitecture *in vivo*. (a) Micro-TENN implant trajectory and dimensions drawn to scale (adapted from Gardoni & Bellone, 2015). (b) Micro-TENN orientation (not to scale). (c) A thick-tissue longitudinal section showing a micro-TENN 15 min following transplantation to span the nigrostriatal pathway and labelled via immunohistochemistry to denote dopaminergic neurons/axons (TH; red). (d) A higher magnification reconstruction from a demonstrative region in (c) depicting both the cell aggregate region and a portion of the axonal region *in vivo*. (e) At 1 week post implant, a representative sagittal section showing a longitudinal view of a dopaminergic micro-TENN with all neurons labelled green (expressing GFP on the synapsin promoter) and labelled via immunohistochemistry to denote dopaminergic neurons/axons (TH; red). This demonstrates that micro-TENN neurons survived and the longitudinally aligned cytoarchitecture was at least partially maintained. (f) At 1 month post implant, a representative oblique section providing a cross-sectional view of a GFP+ dopaminergic micro-TENN (green) labelled via immunohistochemistry to denote dopaminergic neurons/axons (TH; red) and all neurons/axons (β -tubulin III; purple). This demonstrates healthy transplanted neurons/axons with robust dopaminergic axonal projections at 1 month *in vivo*. Scale bar (c,d) = 100 μ m. Scale bar (e) = 20 μ m. Scale bar (f) = 50 μ m [Colour figure can be viewed at wileyonlinelibrary.com]

transplantation, as glutamate is coreleased with dopamine in some cases (Broussard, 2012). However, if we find that a higher purity of dopaminergic neurons is necessary for functional efficacy, then we could use a later developmental time point for midbrain isolation (Pothos, Davila, & Sulzer, 1998), cell sorting, and/or differentiation from stem cell sources, all of which have been shown to further enrich dopaminergic populations.

Our method to plate micro-TENN with dopaminergic “aggregates” alleviated the lack of separation between the neuronal somata and neurites that we observed in some cases when micro-TENN were plated with dissociated cells. It was particularly important to ensure that the micro-TENN demonstrated the desired cytoarchitecture of a discrete cell body region projecting axons through the length of the inner core because separate somatic and axonal regions is a key feature of

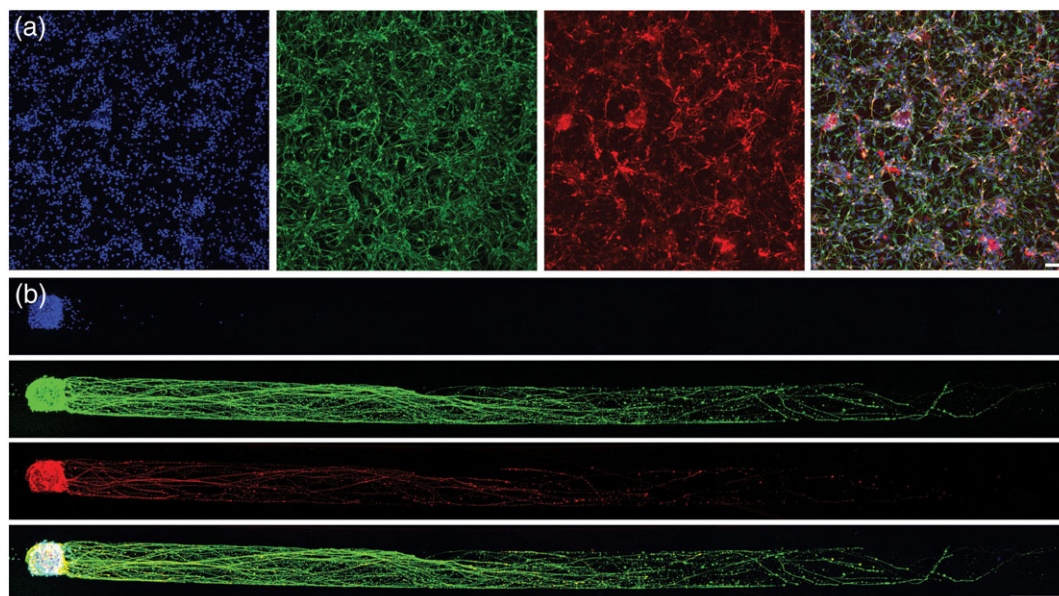


FIGURE 8 Microtissue engineered neural networks (micro-TENNs) generated with human embryonic stem cell-derived dopaminergic neurons. H9 human embryonic stem cells were differentiated into dopaminergic neurons and labelled via immunocytochemistry to denote all neurons/axons (β -tubulin III; green) and dopaminergic neurons/axons (TH; red), with nuclear counterstain (Hoechst; blue). (a) Differentiated dopaminergic neurons shown in two-dimensional culture. (b) Differentiated dopaminergic neurons were dissociated, aggregated, and inserted into microcolumns, where they extended robust processes measuring over 4 mm by 14 days post plating. Scale bar (a) = 100 μ m. Scale bar (b) = 225 μ m [Colour figure can be viewed at wileyonlinelibrary.com]

the nigrostriatal pathway. We believe that better approximation of the cytoarchitecture of the nigrostriatal pathway will lead to improved functional outcomes following micro-TENN implantation to reconstruct the degenerated dopaminergic neurons in the SNpc and their projections to the striatum. In particular, the dopaminergic neurons in the SNpc synapse directly onto striatal neurons without exerting their effects through intermediate synapses and/or neurons. Therefore, in order for the connectivity and timing of our micro-TENNs to be correct upon integration with the host, our micro-TENNs will likely need to achieve modulation of striatal neurons by propagating signals from the SNpc through a mono-synaptic pathway. Because we were able to create dopaminergic micro-TENNs that approximate the architecture of the nigrostriatal pathway, this increases the likelihood that functional integration *in vivo* will emulate the native mono-synaptic pathway.

By utilizing the neuronal aggregates as well as optimizing the inner core ECM, we confirmed that the micro-TENNs were capable of spanning the length of the nigrostriatal pathway in rats, which is approximately 6 mm. In fact, as far as we know, our micro-TENNs exhibit the longest *in vitro* dopaminergic axonal outgrowth recorded in the literature (Blakely et al., 2011; Denis-Donini, Glowinski, & Prochiantz, 1983; Li et al., 2003; Lin & Isacson, 2006; Nakamura, Ito, Shirasaki, & Murakami, 2000; Park et al., 2006; Shim et al., 2004; Tonges et al., 2012; Wakita et al., 2010; Yue et al., 1999; Zhang et al., 2004). The dopaminergic cell aggregates produced neurite outgrowth that was approximately 10 \times longer than projections from individual cells. This may be influenced by the fact that the cellular density within the neuronal aggregates is more representative of the density within the brain. This higher cell density may have given the aggregated neurons better control over their 3D microenvironment than dissociated cells, which in turn promoted better cell viability and health and therefore enhanced axonal extension. Moreover, the gene expression of cells in the aggregates may also be more representative of cells in the

brain and allows the cells to tap into developmental programs to initiate axonal outgrowth (Ungrin et al., 2008). Furthermore, many neuronal subtypes are programmed for either short or long distance communication (Caputi, Melzer, Michael, & Monyer, 2013). In dissociated micro-TENNs, "long distance" axons likely meet synaptic partners at intermediate distances along the length of the microcolumn. In contrast, for the aggregate micro-TENNs, the absence of any intermediate neighbours may have prompted the long distance neurons to up-regulate proteins for long distance outgrowth and thus project the length of the microcolumns. Lastly, the aggregates give rise to grouped and fasciculated axonal projections, which may produce a sustained drive for axonal extension due to concentrated and persistent progrowth signalling, and/or physical/structural advantages. The rates and lengths of dopaminergic axonal extension from the neuronal aggregates were unprecedented, although clearly, further studies are required to elucidate the mechanisms of ultralong axonal projections from the aggregates.

In our attempts to maximize axonal outgrowth, we found that collagen I and a collagen I + laminin cocktail produced the longest outgrowth when used as the biomaterial for the inner core. We believe this occurred because, unlike the laminin coating and empty cores, the collagen I and collagen I + laminin cocktail both provided a continuous, 3D scaffold that supported axonal outgrowth. Although the crosslinked collagen also provided a continuous scaffold, it was much stiffer and likely more resistive to enzymatic degradation upon growth cone extension. Interestingly, utilizing media enriched in growth factors did not increase axonal outgrowth. As engineered growth factor gradients were not employed, our results suggest that the axons may be relatively nonresponsive to global changes in growth signals. Likewise, neither the use of a dopaminergic neuron aggregate nor the use of a striatal neuron aggregate surrogate end target increased axonal outgrowth, which does not support our hypothesis that chemotactic cues generated from an end target would accelerate axonal

outgrowth. Potentially, suprathreshold peak growth factor concentrations and adequate chemotactic gradients could not be established due to the significant diffusional distance (1.2 cm) required to span the two populations.

While investigating the *in vitro* functionality of the dopaminergic micro-TENNs, we used FSCV to confirm that our micro-TENNS could release dopamine both within the neuronal aggregate and at the axon terminals. The FSCV experiments were performed within scaled up micro-TENNs to allow for ease of access for stimulating and recording electrodes. Likewise, although the micro-TENNs were incubated in media containing L-DOPA in order to amplify the dopamine signal for ease of detection, our ability to record evoked dopamine release demonstrates that the machinery necessary for dopamine synthesis and release was present. Allowing the dopaminergic neurons within the micro-TENNs to mature in culture was crucial, as it was difficult to record dopamine release at earlier time points (data not shown). Although the cyclic voltammograms demonstrated oxidation between 0.55 and 0.65 V and reduction between -0.20 and -0.30 V, which are characteristic of dopamine (Heien et al., 2003), the voltammograms also exhibited an oxidation peak around 0 V. We believe this additional peak is a result of the release of neurotransmitters from nondopaminergic neurons present in our impure midbrain populations.

Our *in vitro* test bed to investigate the micro-TENNS' ability to synapse with an aggregate of striatal cells revealed extensive synaptic labelling in areas where the dopaminergic micro-TENN axons grew into the striatal neurons. These findings suggest that the dopaminergic axons integrated with the striatal neuron population and provides proof-of-concept for our tissue engineered nigrostriatal pathway *in vitro*. However, higher resolution tract tracing, transsynaptic markers and/or electrophysiological measures will be required in the future to confirm functional integration in this test bed.

Animals sacrificed immediately following injection of micro-TENNS to span the nigrostriatal pathway revealed that the transplantation process itself did not alter the cytoarchitecture of the micro-TENNS. Furthermore, at 1 week and 1 month following injection of GFP+ micro-TENNS, evidence of micro-TENN survival and maintenance of cytoarchitecture was found. Specifically, surviving GFP+ and TH+ neurons were located within the lumen along the injection trajectory. Out to 1 month post implant, histological sections orthogonal to the implant trajectory revealed dense GFP+ neurons/axons and TH+ axons in cross-section within the microcolumn. Although these findings are sufficient to demonstrate proof-of-concept for the implant paradigm and neuronal survival *in vivo*, future chronic studies will utilize immune suppressed animals in order to mitigate potential loss of transplanted neurons/axons due to host immune responses. In addition, the circuitry of the nigrostriatal pathway is complex, and although the linear trajectory of implantation was adequate to physically span the substantia nigra and striatum, our implantation trajectory may be refined in future studies using curved micro-TENNS to take into account relevant substructures within these anatomical substrates. Most importantly, it is imperative that the micro-TENNS undergo further testing in a rat model of Parkinson's disease in order to determine their ability to ameliorate motor symptoms and restore dopamine levels in the striatum.

Our proposed strategy may be the first approach capable of simultaneously replacing dopaminergic neurons in the substantia nigra while physically reconstructing their long axonal tracts to the striatum. This

will allow the implanted micro-TENNS to be subject to the normal cellular modulation that dopaminergic SNpc neurons are subject to *in vivo* to "close the loop" and restore a crucial circuit for motor control feedback. Our process to generate micro-TENNS enables a precisely engineered structure where the number of neurons and generation of dopamine can be known prior to implantation. Furthermore, in principle, our method surpasses graft and cell-based methods by simultaneously restoring neurons and their long-distance axons to the striatum. In order to supply the 80,000 dopaminergic cells and >3.0 cm axonal lengths needed for functional improvement in humans, our micro-TENNS will eventually need to be scaled up considerably for clinical trials. As a first step towards this benchmark, our successful generation of micro-TENNS using dopaminergic neurons derived from hESCs demonstrates feasibility of using human cell sources. In the future, we foresee the generation of autologous micro-TENNS using cellular reprogramming techniques, which may eliminate the need for immunosuppression (Swistowski et al., 2010). Although it is possible that these autologous micro-TENNS would eventually degenerate similar to native tissue, previous research has shown that dopaminergic neurons from tissue grafts can survive decades *in vivo* despite ongoing degeneration of the native dopaminergic system (Cai, Peng, Nelson, Eberhart, & Smith, 2005; Kim, Haftel, Kumar, & Bellamkonda, 2008). Furthermore, we envision the development of Parkinson's disease-resistant micro-TENNS via genetic approaches to minimize α -synuclein (the primary pathological protein in Parkinson's disease) induced pathology to lengthen the micro-TENN lifespan. Thus, as micro-TENNS are more targeted than systemically delivered drugs, have a smaller form factor than DBS electrodes, and provide the opportunity to reconstruct lost neuroanatomy, they have the potential to revolutionize Parkinson's disease treatment and dramatically improve patient outcomes.

ACKNOWLEDGEMENTS

Financial support was provided by the Michael J. Fox Foundation [Therapeutic Pipeline Program #9998 (Cullen)], the Department of Veterans Affairs [BLR&D Merit Review I01-BX003748 (Cullen)], the National Institutes of Health [U01-NS094340 (Cullen), R01-DA031900 (España), T32-NS091006, F31-DA042505 (Brodnik) & T32-NS043126 (Harris)], Penn Medicine Neuroscience Center Pilot Award (Cullen), and the National Science Foundation [Graduate Research Fellowship DGE-1321851 (Struzyna)].

AUTHOR CONTRIBUTIONS

L.A.S. fabricated the micro-TENNS, performed the *in vitro* optimization and microscopy, designed experiments, performed data analysis, prepared figures, and prepared the manuscript. D.K.C. conceived the study and assisted with experimental design, data analysis, and manuscript preparation. K.D.B. and J.C.B. performed the transplant surgeries, conducted the histological analysis, and assisted with figure preparation. R.A.E. and Z.D.B. performed the FSCV experiments, analysed the FSCV data, and assisted with figure preparation. J.P.H. assisted with figure preparation and experimental design. H.I.C., J.A.W., and J.E.D. contributed to the experimental design and data analysis. J.L. assisted with the stem cell culture and differentiation. K.V.P. provided technical assistance in these studies. K.D.B., J.C.B., R.A.E., Z.D.B., J.P.H., H.I.C., J.A.W., and J.E.D. provided critical feedback on the manuscript.

CONFLICT OF INTEREST

D.K.C. is a scientific co-founder of INNERVACE, LLC, and Axonova Medical, LLC, which are University of Pennsylvania spin-out companies focused in neuroregenerative medicine. No other author has declared a potential conflict of interest.

ORCID

Laura A. Struzyna  <http://orcid.org/0000-0003-0201-7896>

REFERENCES

- Bjorklund, A., & Lindvall, O. (2000). Cell replacement therapies for central nervous system disorders. *Nature Neuroscience*, 3(6), 537–544.
- Blakely, B. D., Bye, C. R., Fernando, C. V., Horne, M. K., Macheda, M. L., Stackner, S. A., ... Parish, C. L. (2011). Wnt5a regulates midbrain dopaminergic axon growth and guidance. *PLoS One*, 6(3), e18373.
- Borisoff, J. F., Chan, C. C., Hiebert, G. W., Oschipok, L., Robertson, G. S., Zamboni, R., ... Tetzlaff, W. (2003). Suppression of Rho-kinase activity promotes axonal growth on inhibitory CNS substrates. *Molecular and Cellular Neurosciences*, 22(3), 405–416.
- Broussard, J. I. (2012). Co-transmission of dopamine and glutamate. *The Journal of General Physiology*, 139(1), 93–96.
- Cai, J., Peng, X., Nelson, K. D., Eberhart, R., & Smith, G. M. (2005). Permeable guidance channels containing microfilament scaffolds enhance axon growth and maturation. *Journal of Biomedical Materials Research Part A*, 75(2), 374–386.
- Caputi, A., Melzer, S., Michael, M., & Monyer, H. (2013). The long and short of GABAergic neurons. *Current Opinion in Neurobiology*, 23(2), 179–186.
- Cullen, D. K., Tang-Schomer, M. D., Struzyna, L. A., Patel, A. R., Johnson, V. E., Wolf, J. A., & Smith, D. H. (2012). Microtissue engineered constructs with living axons for targeted nervous system reconstruction. *Tissue Engineering Part A*, 18(21–22), 2280–2289.
- Dauer, W., & Przedborski, S. (2003). Parkinson's disease: Mechanisms and models. *Neuron*, 39(6), 889–909.
- Davie, C. A. (2008). A review of Parkinson's disease. *British Medical Bulletin*, 86, 109–127.
- Denis-Donini, S., Glowinski, J., & Prochiantz, A. (1983). Specific influence of striatal target neurons on the in vitro outgrowth of mesencephalic dopaminergic neurites: A morphological quantitative study. *The Journal of Neuroscience: The Official Journal of the Society for Neuroscience*, 3(11), 2292–2299.
- Freed, C. R., Greene, P. E., Breeze, R. E., Tsai, W. Y., DuMouchel, W., Kao, R., ... Fahn, S. (2001). Transplantation of embryonic dopamine neurons for severe Parkinson's disease. *The New England Journal of Medicine*, 344(10), 710–719.
- Gardoni, F., & Bellone, C. (2015). Modulation of the glutamatergic transmission by Dopamine: A focus on Parkinson, Huntington and Addiction diseases. *Frontiers in Cellular Neuroscience*, 9, 25.
- Grealish, S., Diguett, E., Kirkeby, A., Mattsson, B., Heuer, A., Bramoulle, Y., ... Parmar, M. (2014). Human ESC-derived dopamine neurons show similar preclinical efficacy and potency to fetal neurons when grafted in a rat model of Parkinson's disease. *Cell Stem Cell*, 15(5), 653–665.
- Harris, J. P., Struzyna, L. A., Murphy, P. L., Adewole, D. O., Kuo, E., & Cullen, D. K. (2016). Advanced biomaterial strategies to transplant preformed micro-tissue engineered neural networks into the brain. *Journal of Neural Engineering*, 13(1), 016019.
- Heien, M. L., Phillips, P. E., Stuber, G. D., Seipel, A. T., & Wightman, R. M. (2003). Overoxidation of carbon-fiber microelectrodes enhances dopamine adsorption and increases sensitivity. *The Analyst*, 128(12), 1413–1419.
- Hyman, C., Hofer, M., Barde, Y. A., Juhasz, M., Yancopoulos, G. D., Squinto, S. P., & Lindsay, R. M. (1991). BDNF is a neurotrophic factor for dopaminergic neurons of the substantia nigra. *Nature*, 350(6315), 230–232.
- Katzenschlager, R., & Lees, A. J. (2002). Treatment of Parkinson's disease: Levodopa as the first choice. *Journal of Neurology*, 249(Suppl 2), II19–II24.
- Kim, H. J. (2011). Stem cell potential in Parkinson's disease and molecular factors for the generation of dopamine neurons. *Biochimica et Biophysica Acta*, 1812(1), 1–11.
- Kim, Y. T., Haftel, V. K., Kumar, S., & Bellamkonda, R. V. (2008). The role of aligned polymer fiber-based constructs in the bridging of long peripheral nerve gaps. *Biomaterials*, 29(21), 3117–3127.
- Kriks, S., Shim, J. W., Piao, J., Ganat, Y. M., Wakeman, D. R., Xie, Z., ... Studer, L. (2011). Dopamine neurons derived from human ES cells efficiently engraft in animal models of Parkinson's disease. *Nature*, 480(7378), 547–551.
- Li, F. Q., Cheng, X. X., Liang, X. B., Wang, X. H., Xue, B., He, Q. H., ... Han, J. S. (2003). Neurotrophic and neuroprotective effects of triphlorolide, an extract of Chinese herb *Tripterygium wilfordii* Hook F, on dopaminergic neurons. *Experimental Neurology*, 179(1), 28–37.
- Lin, L., & Isacson, O. (2006). Axonal growth regulation of fetal and embryonic stem cell-derived dopaminergic neurons by Netrin-1 and Slits. *Stem Cells*, 24(11), 2504–2513.
- Merz, G., Schwenk, V., Shah, R. G., Necaie, P., & Salafia, C. M. (2017). Clarification and 3-D visualization of immunolabeled human placenta villi. *Placenta*, 53, 36–39.
- Moore, M. J., Friedman, J. A., Lewellyn, E. B., Mantila, S. M., Krych, A. J., Ameenuddin, S., ... Yaszemski, M. J. (2006). Multiple-channel scaffolds to promote spinal cord axon regeneration. *Biomaterials*, 27(3), 419–429.
- Moro, E., Lozano, A. M., Pollak, P., Agid, Y., Rehncrona, S., Volkmann, J., ... Lang, A. E. (2010). Long-term results of a multicenter study on subthalamic and pallidal stimulation in Parkinson's disease. *Movement Disorders: Official Journal of the Movement Disorder Society*, 25(5), 578–586.
- Nakamura, S., Ito, Y., Shirasaki, R., & Murakami, F. (2000). Local directional cues control growth polarity of dopaminergic axons along the rostrocaudal axis. *The Journal of Neuroscience: The Official Journal of the Society for Neuroscience*, 20(11), 4112–4119.
- Nikkhah, G., Cunningham, M. G., Cenci, M. A., McKay, R. D., & Bjorklund, A. (1995). Dopaminergic microtransplants into the substantia nigra of neonatal rats with bilateral 6-OHDA lesions. I. Evidence for anatomical reconstruction of the nigrostriatal pathway. *The Journal of Neuroscience: The Official Journal of the Society for Neuroscience*, 15(5 Pt 1), 3548–3561.
- Obeso, J. A., Rodriguez-Oroz, M. C., Goetz, C. G., Marin, C., Kordower, J. H., Rodriguez, M., ... Halliday, G. (2010). Missing pieces in the Parkinson's disease puzzle. *Nature Medicine*, 16(6), 653–661.
- Olanow, C. W., Freeman, T., & Kordower, J. (2001). Transplantation of embryonic dopamine neurons for severe Parkinson's disease. *The New England Journal of Medicine*, 345(2), 146. author reply 147
- Park, C. H., Kang, J. S., Shin, Y. H., Chang, M. Y., Chung, S., Koh, H. C., ... Lee, S. H. (2006). Acquisition of in vitro and in vivo functionality of Nurr1-induced dopamine neurons. *FASEB Journal: Official Publication of the Federation of American Societies for Experimental Biology*, 20(14), 2553–2555.
- Pothos, E. N., Davila, V., & Sulzer, D. (1998). Presynaptic recording of quanta from midbrain dopamine neurons and modulation of the quantal size. *The Journal of Neuroscience: The Official Journal of the Society for Neuroscience*, 18(11), 4106–4118.
- Pruszk, J., Just, L., Isacson, O., & Nikkhah, G. (2009). Isolation and culture of ventral mesencephalic precursor cells and dopaminergic neurons from rodent brains. *Current Protocols in Stem Cell Biology*. Chapter 2: Unit 2D 5
- Redmond, D. E. Jr., Sladek, J. R., & Spencer, D. D. (2001). Transplantation of embryonic dopamine neurons for severe Parkinson's disease. *The New England Journal of Medicine*, 345(2), 146–147.
- Shim, J. W., Koh, H. C., Chang, M. Y., Roh, E., Choi, C. Y., Oh, Y. J., ... Lee, S. H. (2004). Enhanced in vitro midbrain dopamine neuron differentiation, dopaminergic function, neurite outgrowth, and 1-methyl-4-phenylpyridium resistance in mouse embryonic stem cells overexpressing Bcl-XL. *The Journal of Neuroscience: The Official Journal of the Society for Neuroscience*, 24(4), 843–852.
- Silva, N. A., Salgado, A. J., Sousa, R. A., Oliveira, J. T., Pedro, A. J., Leite-Almeida, H., ... Reis, R. L. (2010). Development and characterization

- of a novel hybrid tissue engineering-based scaffold for spinal cord injury repair. *Tissue Engineering Part A*, 16(1), 45–54.
- Struzyna, L. A., Harris, J. P., Katiyar, K. S., Chen, H. I., & Cullen, D. K. (2015). Restoring nervous system structure and function using tissue engineered living scaffolds. *Neural Regeneration Research*, 10(5), 679–685.
- Struzyna, L. A., Katiyar, K. K., & Cullen, D. K. (2014). Living scaffolds for neuroregeneration. *Current Opinion in Solid State & Materials Science*, 18(6), 308–318.
- Struzyna, L. A., Wolf, J. A., Mietus, C. J., Adewole, D. O., Chen, H. I., Smith, D. H., & Cullen, D. K. (2015). Rebuilding brain circuitry with living micro-tissue engineered neural networks. *Tissue Engineering Part A*, 21(21–22), 2744–2756.
- Swistowski, A., Peng, J., Liu, Q., Mali, P., Rao, M. S., Cheng, L., & Zeng, X. (2010). Efficient generation of functional dopaminergic neurons from human induced pluripotent stem cells under defined conditions. *Stem Cells*, 28(10), 1893–1904.
- Thompson, L. H., Grealish, S., Kirik, D., & Björklund, A. (2009). Reconstruction of the nigrostriatal dopamine pathway in the adult mouse brain. *European Journal of Neuroscience*, 30(4), 625–638.
- Tonges, L., Frank, T., Tatenhorst, L., Saal, K. A., Koch, J. C., Szego, E. M., ... Lingor, P. (2012). Inhibition of rho kinase enhances survival of dopaminergic neurons and attenuates axonal loss in a mouse model of Parkinson's disease. *Brain: A Journal of Neurology*, 135(Pt 11), 3355–3370.
- Ungrin, M. D., Joshi, C., Nica, A., Bauwens, C., & Zandstra, P. W. (2008). Reproducible, ultra high-throughput formation of multicellular organization from single cell suspension-derived human embryonic stem cell aggregates. *PLoS One*, 3(2), e1565.
- Wakita, S., Izumi, Y., Matsuo, T., Kume, T., Takada-Takatori, Y., Sawada, H., & Akaïke, A. (2010). Reconstruction and quantitative evaluation of dopaminergic innervation of striatal neurons in dissociated primary cultures. *Journal of Neuroscience Methods*, 192(1), 83–89.
- Weinert, M., Selvakumar, T., Tierney, T. S., & Alavian, K. N. (2015). Isolation, culture and long-term maintenance of primary mesencephalic dopaminergic neurons from embryonic rodent brains. *Journal of visualized experiments: JoVE*. (96)
- Yorgason, J. T., España, R. A., & Jones, S. R. (2011). Demon voltammetry and analysis software: Analysis of cocaine-induced alterations in dopamine signaling using multiple kinetic measures. *Journal of Neuroscience Methods*, 202(2), 158–164.
- Yue, Y., Widmer, D. A., Halladay, A. K., Cerretti, D. P., Wagner, G. C., Dreyer, J. L., & Zhou, R. (1999). Specification of distinct dopaminergic neural pathways: Roles of the Eph family receptor EphB1 and ligand ephrin-B2. *The Journal of Neuroscience: The Official Journal of the Society for Neuroscience*, 19(6), 2090–2101.
- Zhang, L., Fletcher-Turner, A., Marchionni, M. A., Apparsundaram, S., Lundgren, K. H., Yurek, D. M., & Seroogy, K. B. (2004). Neurotrophic and neuroprotective effects of the neuregulin glial growth factor-2 on dopaminergic neurons in rat primary midbrain cultures. *Journal of Neurochemistry*, 91(6), 1358–1368.

SUPPORTING INFORMATION

Additional supporting information may be found online in the Supporting Information section at the end of the article.

Figure S1: Dissociated Ventral Mesencephalon Neurons in Planar Culture and Within Micro-Columns. Neuronal cultures labeled via immunocytochemistry to denote all neurons/axons (β -tubulin III; green) and dopaminergic neurons/axons (TH; red), with nuclear counterstain (Hoechst; blue). (A–C) Dopaminergic neurons in planar culture showing significant neurite outgrowth and random network formation out to 28 DIV. (D–G) Representative micro-TENN at 7 DIV initially plated

as a cell suspension. The single cell suspension infiltrated the length of the inner core of the micro-column and did not demonstrate the desired cytoarchitecture requiring separate cell body and axonal regions. (H1–H3) Higher magnification reconstructions from demonstrative regions in (D–G). Neurons and neurites present in a micro-TENN plated with a cell suspension show a lack of organization and directionality. Scale bar (C) = 250 μ m. Scale bar (G) = 200 μ m. Scale bar (H3) = 125 μ m.

Figure S2: Chance Cell Aggregation in Micro-TENNs. Micro-TENNs plated with single cell suspensions labeled via immunocytochemistry to denote all neurons/axons (β -tubulin III; green) and dopaminergic neurons/axons (TH; red), with nuclear counterstain (Hoechst; blue). (A–D) At 14 DIV, a micro-TENN showed the desired cytoarchitecture due to chance re-aggregation of the dissociated neurons. (E–H) At 28 DIV, a micro-TENN exhibiting chance re-aggregation of dissociated neurons; however, axonal extension had only reached \sim 2800 μ m in length. (I, J) Higher magnification reconstructions from demonstrative regions in (E–H) showing that chance re-aggregation created discrete regions of (I) cell bodies and (J) axons in some cases. Scale bar (D) = 100 μ m. Scale bar (H) = 250 μ m. Scale bar (I, J) = 125 μ m.

Figure S3: Neuronal Aggregate Fabrication and Planar Outgrowth. (A) A custom-designed, 3D printed mold was used to generate the inverted PDMS wells. (B) Representation of PDMS wells used to aggregate cells. Each individual well measured 4 mm wide by 4 mm long by 3.46 mm deep. (C) An array of PDMS wells inserted into a 12-well culture plate. (D) Concentrated neuronal cell suspensions were pipetted into inverted pyramidal wells. The wells were centrifuged to aggregate the neurons by force, after which the wells were incubated overnight to allow the pelleted cells to adhere to each other. (E) A neuronal aggregate pelleted at the bottom of a custom-fabricated inverted PDMS well. (F) A dopaminergic aggregate plated in planar culture was labeled via immunocytochemistry to denote dopaminergic neurons/axons (TH; purple). Aggregates achieved neurite outgrowth of over 5000 μ m in length by 8 DIV. Scale bar (E) = 150 μ m. Scale bar (F) = 500 μ m.

Figure S4: Effects of Growth Factor Concentration and Target Neuronal Population on Axonal Outgrowth within Micro-TENNs. (A) Micro-TENNs cultured in media containing high growth factor concentrations did not result in longer axonal outgrowth than micro-TENNs cultured using standard media ($n = 14$ micro-TENNs each group; Mann-Whitney test, $p = 0.9851$). (B) Micro-TENNs plated bi-directionally with dopaminergic aggregates on both ends ($n = 14$) did not result in longer axonal outgrowth than micro-TENNs plated uni-directionally ($n = 14$ each group; t-test, $p = 0.5219$). Data are presented as mean \pm standard deviation

How to cite this article: Struzyna LA, Browne KD, Brodnik ZD, et al. Tissue engineered nigrostriatal pathway for treatment of Parkinson's disease. *J Tissue Eng Regen Med*. 2018;1–15. <https://doi.org/10.1002/term.2698>